INSTITUTE OF PLASMA PHYSICS

NAGOYA UNIVERSITY

Effect of Inner Subshell Ionization on
Emission Lines OIV Ions

T. Kato, K. Masai and K. Sato

(Received · Jan. 18, 1985)

IPPJ- 719 Feb. 1985

RESEARCH REPORT

NAGOYA, JAPAN

Effect of Inner Subshell Ionization on Emission Lines of OIV Ions

Takako KATO, Kuniaki MASAI* and Kuninori SATO

(Received - Jan. 18, 1985)

IPPJ - 719 Feb. 1985

Submitted to Physics Letters

Further communication about this report is to be sent to the Research Information Center, Institute of Plasma Physics, Nagoya University, Nagoya, Japan.

Present Address:

* Department of Physics, Nagoya University, Nagoya 464 Japan.

The effect of metastable states on the emission lines of O III, O IV and OV ions were investigated using the spectroscopic data in a tokamak plasma[1,2]. The excited state populations that are predominantly excited from the metastable state have a quadratic dependence on the electron density, n_e. This is in contrast to the case where the states are directly populated by excitation from the ground-state ion. Therefore, the intensity ratio between two such lines is proportional to n_e. Secondly, the excitation from the metastable state to the resonance state becomes significant at high density. Thirdly, the ionization balance of oxygen ions is modified by ionization from the metastable ions. This is because the metastable-state density is sometimes quite high: e.g., the population in the $2s2p\ ^3P$ state of OV becomes higher than that of the ground $2s^2\ ^1S$ state when $n_e > 10^{12} cm^{-3}$.

In our recent experiment we have found evidence that the metastable states of O IV and OV ions are substantially populated directly through ionization of the inner subshell electrons of the lower-ionization-stage ions.

Several line intensities of OIV and OV ions were measured on the JIPPT-IIU tokamak plasma along the central-chord by using a grazing-incidence monochromator (grating with 600 lines mm^{-1}, grazing incidence angle of 86°, entrance and exit slit widths of 10 and 20 μm, respectively, and the resolution of 0.2 A), equipped with an electron multiplier with a CsI coated photocathode. The relative spectral sensitivity of the monochromator had been calibrated by the branching ratio method

using several VUV line pairs of impurities in the same tokamak plasma. The wavelengths and the transitions of the observed lines are listed in Table I : these lines are referred to by symbols I_r, I_i and I_t in Fig. 1 and Table I. Line intensity ratios between these lines were obtained during ohmic heating: the data acquisition period was between 80 and 100 ms, when the plasma was quite stationary, after the initiation of the plasma. Figures 2 - 4 show some examples of the observed line intensity ratios for 2 series of experiment separated by two weeks.

We solve the coupled equations for the populations of the levels having the principal quantum number n = 2 of the OI - OIX ions in stationary conditions[2] as follows:

$$\sum_j (C_{ji} n_e + A_{ji}) n_j - \sum_j (C_{ij} n_e + A_{ij}) n_i - (\sum_l S_{il} + \sum_m R_{im}) n_e n_i + \sum_m S_{mi} n_e n_m + \sum_l R_{li} n_e n_l = 0, \quad i = 1,2,\ldots N \qquad (1)$$

where n_i is the population density of the i-th levels, C_{ji} and A_{ji} are the excitation rate coefficient and the transition probability; R_{im} is the recombination rate coefficient from the i-th level to the m-th level of the next lower ionized ion and S_{il} is the ionization rate coefficient from the i-th level to the l-th level of the next higher ionized ion.

As the diffusion process is not negligible in a tokamak plasma, it is necessary to add the diffusion term to eq.(1). But in order to see the contribution of the inner subshell ionization directly as will be discussed later, we introduce parameters $p = n_1(\mathrm{OIV})/n_1(\mathrm{OV})$ and $q = n_1(\mathrm{OIII})/n_1(\mathrm{OIV})$, where

n_1 means the population density of the ground state. For a given value p, the rate equation (1) are solved for N-2 variables omitting two equations corresponding to the level numbers of n_1(OIV) and n_1(OV). This means that the plasma is not ionization equilibrium. As the relaxation time of ionization is much shorter than the time scale of a tokamak, the stationary condition for the ground states of other ions is satisfied.

The energy level diagrams for OIII, OIV and OV are shown in Fig. 1. The collisional transitions by electron impact are indicated by solid lines, and the radiative transitions by dashed lines. For the excitation rate coefficints direct to the upper levels for I_r, I_i and I_t of OIV and OV ions we adopt the data evaluated by Itikawa et al[3]. For the excitation rate coefficients of other transitions, level energies and transition probabilities we employ the theoretical results of Bhatia et al[4]. for OIII, Flower and Nussbaumer[5] for OIV and Dufton et al[6]. for OV. We use Lotz's formula[7] for the ionization rate coefficients from both the outer and inner subshell ionization. The radiative and dielectronic recombination rates from the ground state are calculated from Aldrovandi and Pequignot[8].

It is well known that the state of low-ionized impurity ions in tokamak plasmas is predominantly in an ionizing phase owing to its transport motion; in this case the local electron temperature T_e is higher than that expected from ionization equilibrium of the ion species concerned[9,10]. (e.g., if the plasma were in ionization equilibrium, T_e would be only 20 eV

for $n_1(OIV)/n_1(OV) = 1$) Therefore, excited states are populated predominantly through excitation from the low-lying levels, and populating through the higher-lying levels may well be neglected. In this circumstance, T_e is obtained from the ratio of the populations of excited states of ions at the same ionization stage, e.g. from I_t/I_r of OIV or OV. The electron temperature thus obtained experimentally is 100 eV from OIV and 150 eV from OV. This difference appears to reflect the radial dependence of T_e and different distributions of the OIV and OV ions.

Under the ionizing plasma condition the ratio $I_r(OV)/I_r(OIV)$ is almost directly proportional to the density ratio $n_1(OV)/n_1(OIV)$ as shown in Fig. 2 for several cases with different n_e and T_e. The deviation from the linear dependence at high n_e and low $n_1(OV)$, shown by dotted lines, is due to the excitation of the OV $2s2p\ ^1P$ from the metastable state $2s2p\ ^3P$. Comparison with the experimental values leads to the ratio $n_1(OV)/n_1(OIV)$ of 1.3. This conclusion is almost independent of the temperature.

Figure 3 shows the density dependence of the ratio $I_i(OV)/I_r(OV)$. First, we look at the curve with p = 0 ($S_{j1} = S_{mj} = 0$ and $R_{jm} = R_{1j} = 0$ for a excited level j). The upper state of I_i, $2p^2\ ^3P$, is populated only through excitation from the matastable $2s2p\ ^3P$ state. This is because the excitation from the ground state, $2s^2\ ^1S$, is two-electron excitation with spin exchange and should have a small cross section. The metastable state, in turn, is excited from the

ground state and its population is proportional to n_e. The direct excitation to $2p^2\ ^3P$ from the ground state can be neglected for $n_e > 10^9$ cm^{-3}. Thus the intensity ratio I_i/I_r is proportional to n_e until n_e is so high that the metastable state population saturates. This saturation occurs when the collisional deexcitation and ionization from the metastable state become faster than the radiative decay. The metastable population in the higher n_e region is balanced between the excitation from the ground state and its inverse plus the ionization and excitation, resulting in a higher population density than the ground-state density. Comparison with our experiment (Fig. 3) indicates that the experimental ratio is too large to be fitted with the present calculation.

Since the excitation from the ground state to the metastable state causes a spin change, its cross section decreases very rapidly with increase in collision energy, while the inner subshell ionization cross section behaves like an excitation cross section of an optically allowed transition. Therefore, in the present case, the latter rate coefficient becomes larger than the former for $T_e > 100$ eV. I_i/I_r decreases for high T_e. Now we introduce the contribution by the inner subshell ionization from $2s^2 2p\ ^2P$ (OIV) to the metastable state $2s2p\ ^3P$ (OV) population. In Fig.3, the intensity ratio $I_i(\mathrm{OIV})/I_r(\mathrm{OIV})$ are given for $p = 1$ and 0.8. From Fig.2 we had $p \approx 0.8$ and, if we assume this value, our experimental ratio is then interpreted as indicating $n_e > 10^{12}$ cm^{-3} for $T_e = 150$ eV.

In the case of OIV, which is shown in Fig. 4, the situation is more complicated; this is because, for the population of the metastable state $2s2p^2\ ^4P$, recombination from the metastable $2s2p\ ^3P$ (OV) may contribute besides the direct excitation from $2s^22p\ ^2P$ (OIV) and the inner subshell ionization from $2s^22p^2\ ^3P$ (OIII), since the population of the $2s2p\ ^3P$ is larger than that of the ground state for $n_e > 10^{12}cm^{-3}$. The solid curve with $q = 0$, $1/p = 0$ corresponds to the case without the contribution from the recombination and the inner subshell ionization. Our experimental ratios lie far above this calculation. The disagreement is beyond the estimated uncertainty of the cross sections and it cannot be ascribed to an experimental error.

First, we consider the contribution from the recombination. If we assume that the recombination rate coefficient from $2s2p\ ^3P$ is equal to that from $2s^2\ ^1S$,[11] and that $1/p = 10$, although this is unrealistically high, we obtain the curve with the dotted line. It may be concluded that its contribution is insignificant especially for low density consistent with the present ionizing-plasma assumption.

For the inner subshell ionization $2s^22p^2\ ^3P$ (OIII) $\rightarrow 2s2p^2$ (OIV)[12], we have assigned the rate coefficients to $2s2p^2\ ^2P$ and to $2s2p^2\ ^4P$ according to their statistical weights. The populations in the OIV ion are calculated by assuming several values for $q = n_1(\text{OIII})/n_1(\text{OIV})$. Figure 4 shows the results with dash-dotted lines, where $1/p = 0$ is assumed(without recombination from the excited state: $R_{1i} = 0$). From the

observed ratios, we obtain $n_e > 10^{12} cm^{-3}$ for $q = 1$.

We have assumed the uniform temperature and density and neglected transitions between high-lying levels. However, removal of the former assumption and inclusion of these transitions would not alter the present conclusion that our experimental result cannot be interpreted without introducing the inner subshell ionization to the metastable states.

The contribution of the inner subshell ionization is measured and confirmed to be significant in the JIPPT-IIU Tokamak plasma. This is a characteristic phenomenon in the ionizing plasma where the electron temperature is higher than the ionization temperature at which the actual ion ratio would exist in ionization equilibrium. This process increases the level populations especially of metastable states. Thus the intensity I_i is significantly increased. The calculation shows that the intensity I_r is also increased by 10% by the inner subshell ionization in a plasma of $T_e = 100$ eV and $n_e = 10^{12}$ cm^{-3}. Spectroscopic observation of OIV and OV ions can thus be used for the diagnosis of the electron density in tokamak plasmas and it arouses an interest in the study of the inner subshell ionization rate.

The authors gratefully aknowledge Professor T. Fujimoto for his encouragements and helpful discussions. They also would like to thank Professors J. Fujita, M. Otsuks and H. Tawara for useful suggestions and discussions. The authors are indebted to the JIPPT-IIU group for providing us the opportunity of measurement.

References

1. Kato,T., Kako,M., Amano,T., Nomura,Y., and Hayakawa,S. 1981, IPPJ-544 (Institute of Plasma Physics, Nagoya)
2. Kato,T., Masai,K. and Mizuno,J. 1983, J.Phys.Soc.Japan, 52, 3019
3. Itikawa,Y. Hara,S. Kato.T. Nakazaki,S., Pindzola,M.S. and Crandall,D.H., 1983 IPPJ-AM-27 (Institute of Plasma Physics, Nagoya, Japan)
4. Bhatia,A.K., Doschek,G.A. and Feldman,U. 1979, Astron. & Astrophys., 76,359.
5. Flower,D.R. and Nussbaumer,H. 1975, Astron. & Astrophys., 45, 145
6. Dufton,P.L., Berrington,K.A. Burke,P.G. and Kingston,A.E. 1978, Astron. & Astrophys., 62, 111
7. Lotz,W., 1967, Ap.J.Suppl. 24, 207
8. Aldrovandi,S.M.V. and Pequignot,D. 1973, Astron. & Astrophys., 251, 137
9. Fujimoto,T. 1979, J. Phys. Soc. Jpn., 47, 273
10. Gabriel,A.H. 1972, Mon. Not. R. ast. Soc., 160, 99
11. Gau,J.N., Hahn,Yukap and Petter,J.A. 1980, J. Quant. Spectrosc. Radiat. Transfer, 23, 131.
12. Younger,S.M. 1982, J. Quan. Spectrosc. Radiat. Transfer, 27, 541.

Figure captions

Fig.1 A schematic energy level diagram for OIII, OIV and OV ions. Measured lines I_r, I_i and I_t are indicated. Solid lines indicate the transition by electron impact, and dashed lines the radiative transitions.

Fig.2 Correlation between $I_r(OV)/I_r(OIV)$ and $n_1(OV)/n_1(OIV)$ for T_e = 20, 100 and 200 eV. Solid lines indicate the results for $n_e = 10^{10}$ cm^{-3}, and the dashed lines for $n_e = 10^{13}$ cm^{-3}. The observed values are given by arrows.

Fig.3 Intensity ratio $I_i(OV)/I_r(OV)$, including the inner subshell ionization from $OIV(2s^2 2p)$ to $OV(2s2p)$, as a function of the electron density for several values of the parameter $p = n_1(OIV)/n_1(OV)$. The elctron temperature is 150 eV. The observed values are indicated by arrows.

Fig.4 Intensity ratio $I_i(OIV)/I_r(OIV)$ as a function of the electron density for T_e = 100 eV. Dot-dash-lines show the results with the contribution of the inner subshell ionization from OIII ions for $q = n_1(OIII)/n_1(OIV)$ = 0.1 and 1.0. The dotted line indicates the result including the recombination from $2s2p\ ^3P(OV)$ for $1/p = n_1(OV)/n_1(OIV)$ = 10. Observed values are given by arrows.

Table I

Observed lines

Ion	Line	Transition	W. L.(A)
OV	I_r	$2s2p(^1P_1)$ - $2s^2(^1S_0)$	629.73
	I_i	$2p^2(^3P_2)$ - $2s2p(^3P_2)$	760.445
	I_t	$2s3p(^1P_1)$ - $2s^2(^1S_0)$	172.17
OIV	I_r	$2s2p^2(^2D_{3/2,5/2})$ - $2s^22p(^2P_{3/2})$	790.1,.2
	I_i	$2p^3(^4S_{3/2})$ - $2s2p^2(^4P_{5/2})$	625.85
	I_t	$2s^23d(^2D_{5/2,3/2})$ - $2s^22p(^2P_{3/2})$	238.57

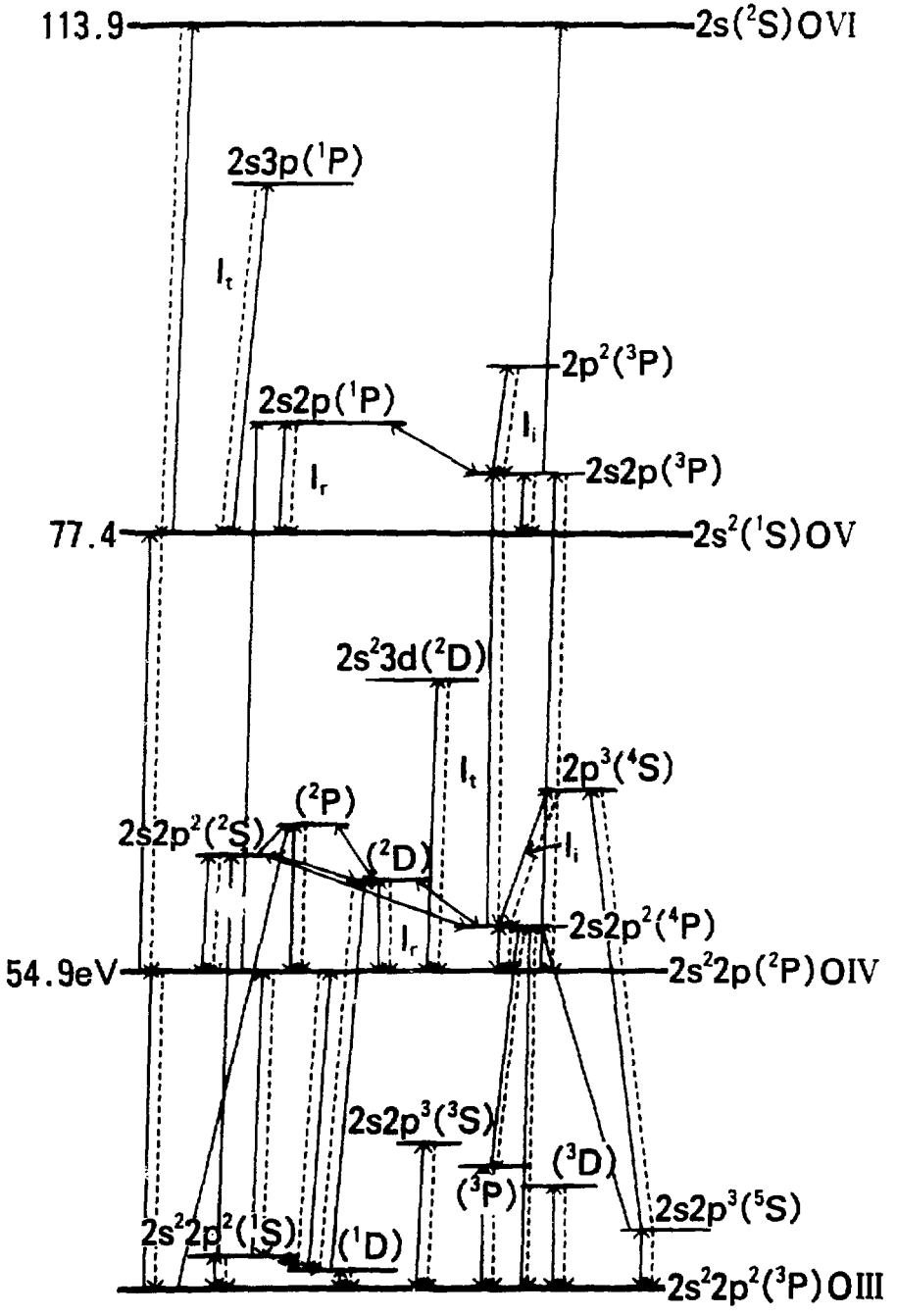
113.9
2s(²S)OVI
2s3p(¹P)
I_t
2p²(³P)
2s2p(¹P)
I_i
I_r
2s2p(³P)
77.4
2s²(¹S)OV
2s²3d(²D)
I_t
2p³(⁴S)
(²P)
2s2p²(²S)
(²D)
I_i
2s2p²(⁴P)
I_r
54.9eV
2s²2p(²P)OIV
2s2p³(³S)
(³D)
(³P)
2s2p³(⁵S)
2s²2p²(¹S)
(¹D)
2s²2p²(³P)OIII

Fig.1

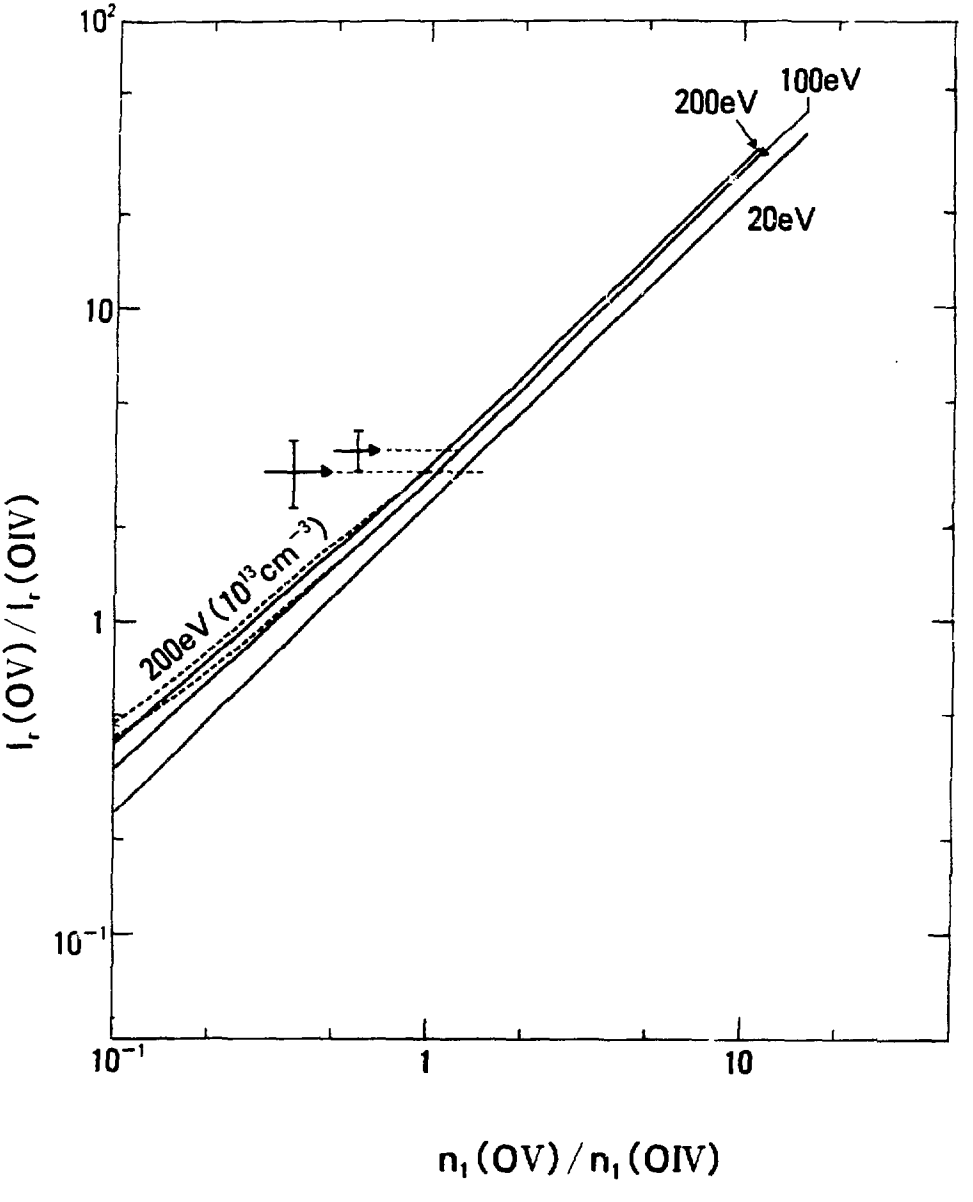
10^2
10
1
10^{-1}
10^{-1}
1
10
100eV
200eV
20eV
200eV (10^{13}cm^{-3})
$I_r(OV)/I_r(OIV)$
$n_1(OV)/n_1(OIV)$

Fig.2

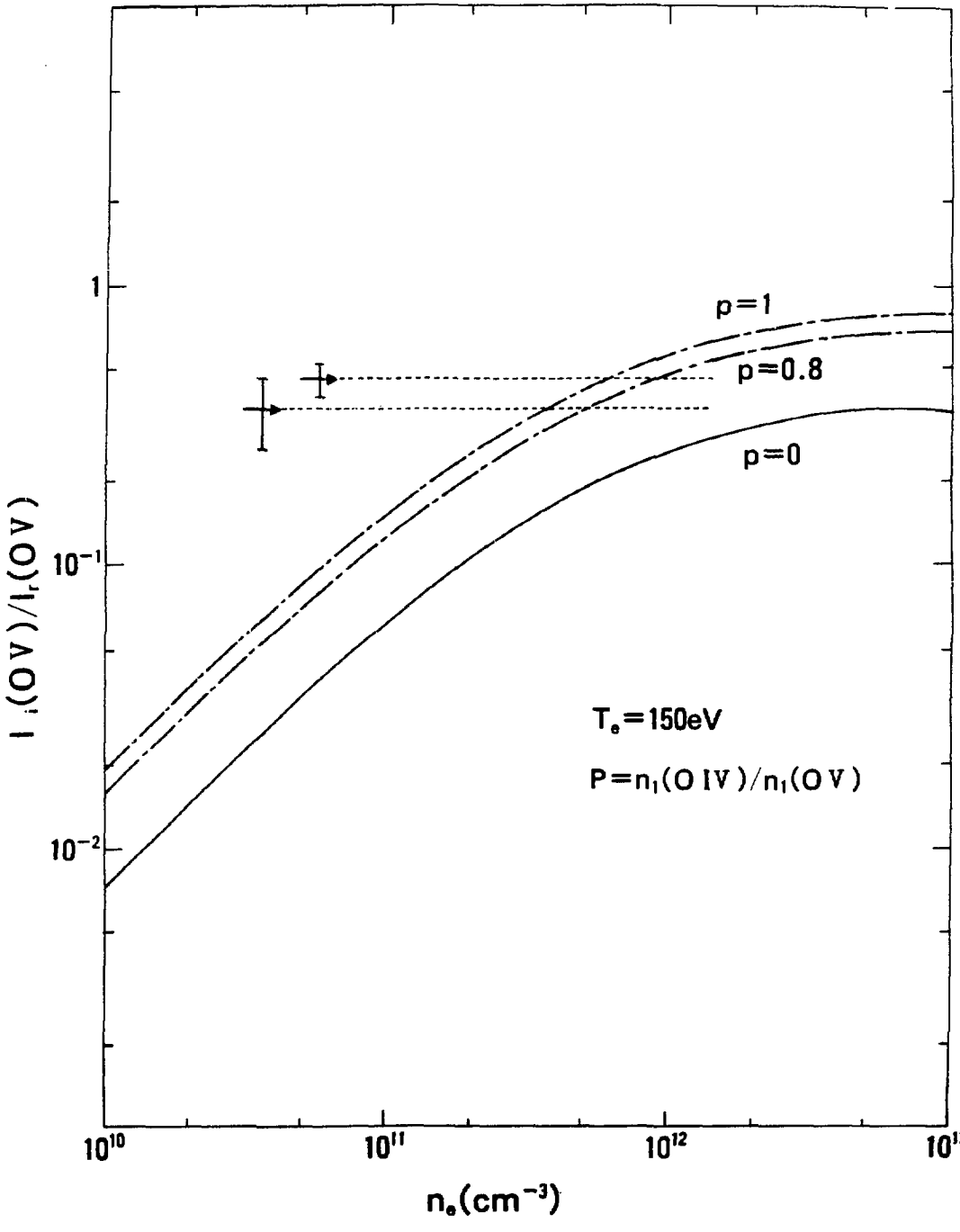
1
10^{-1}
10^{-2}
$I_i(OV)/I_r(OV)$
p=1
p=0.8
p=0
T_e=150eV
P=n_1(O IV)/n_1(O V)
10^{10}
10^{11}
10^{12}
10^{13}
$n_e(cm^{-3})$

Fig.3

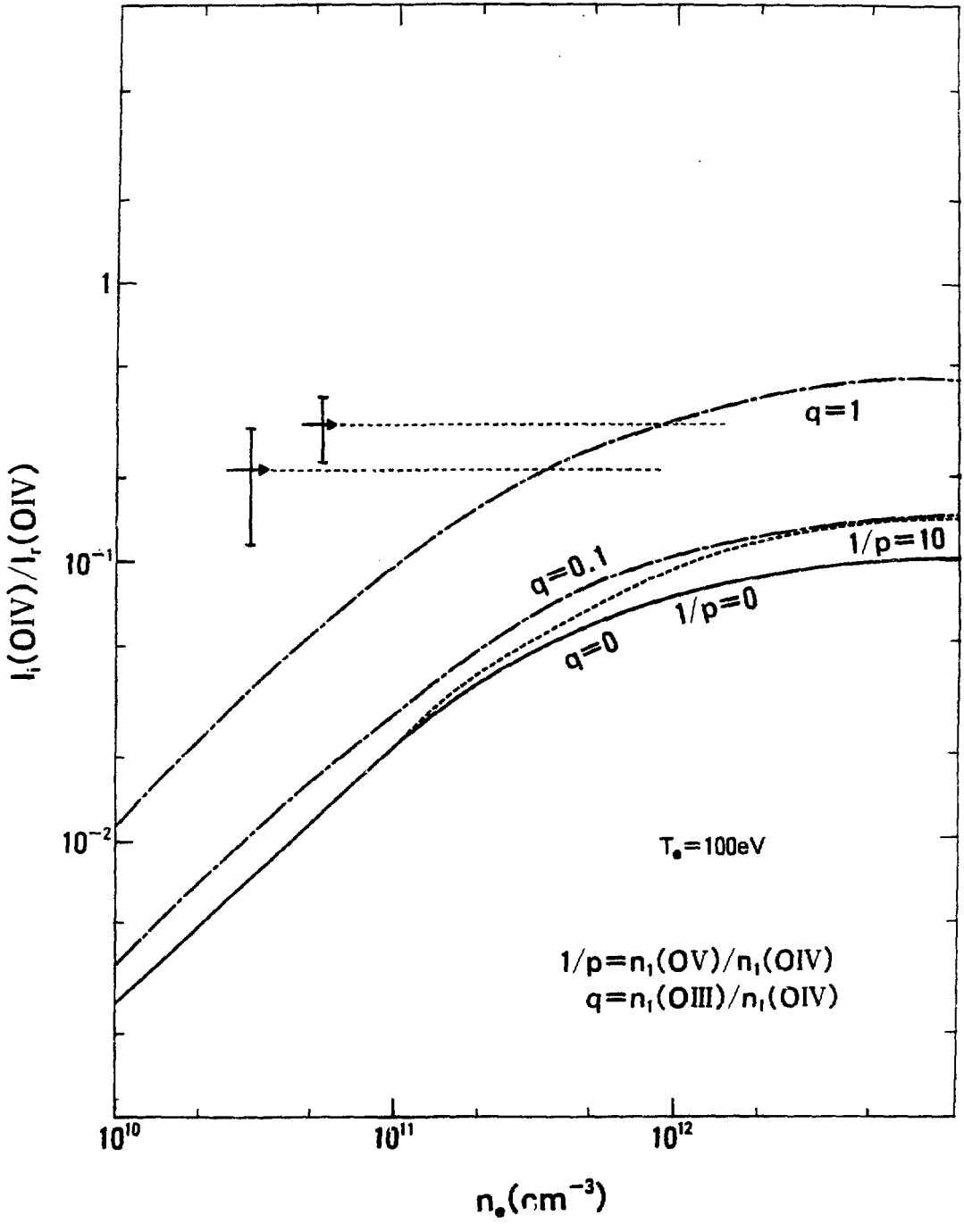
1
10^{-1}
10^{-2}
$I_i(OIV)/I_r(OIV)$
q=1
q=0.1
1/p=10
1/p=0
q=0
T_e=100eV
1/p=$n_1(OV)/n_1(OIV)$
q=$n_1(OIII)/n_1(OIV)$
10^{10}
10^{11}
10^{12}
$n_e(cm^{-3})$

Fig.4